Science in China Ser. D Earth Sciences 2005 Vol.48 Supp. I 225—244

An operational two-layer remote sensing model to estimate surface flux in regional scale: Physical background

ZHANG Renhua, SUN Xiaomin, WANG Weimin, XU Jinping, ZHU Zhilin & TIAN Jing

Institute of Geographic Sciences and Natural Resources Research, Chinese Academy of Sciences, Beijing 100101, China
Correspondence should be addressed to Zhang Renhua (email: zhangrh@igsnrr.ac.cn)

Received July 14, 2004; revised January 19, 2005

Abstract Based on the improved interaction mechanism of two-layer model, this paper proposed Pixel Component Arranging and Comparing Algorithm (PCACA) and theoretically positioning algorithm, estimated the true temperature of mixed pixel in four extreme points in combination with the measurements of dry and wet points in calibration fields and improved the reliability of positioning dry and wet line. A new two-layer energy-separation algorithm was proposed, which was simple and direct without resistance network parameters for each pixel. We also proposed a new thought about the effect of advection. The albedo of mixed pixel was also separated with PCACA. In combination with two-layer energy-separation algorithm, the net radiation of mixed pixel was separated to overcome the uncertainty of conventional energy-separation algorithm using Beer's Law. Through the validation of retrieval result, this method is proved to be feasible and operational. At the same time, the uncertainty of this algorithm was objectively analyzed.

Keywords: two-layer remote sensing model of surface flux in regional scale, PCACA, layered energy-separation algorithm.

DOI: 10.1360/05zd0023

It is well known that currently the techniques to measure the surface flux and related parameters are limited in single point. For the data measured on heterogeneous surface, these measurements could not well represent the real rule of spatial distribution. As a result, the attribute data about regional and global geosciences are often discrete. One of the main reasons for this is that data of a single point were often regarded as that of a certain regional surface in many applications, which makes data inaccurate. In fact, the research about regional surface flux's regulation needs regional and continual 2-D data to reflect truly objective world. So, there is a supply/demand conflict between the measurement ability in point and the need of objective world. This conflict is a rigorous challenge.

More and more attention has been paid to the retrieval method of surface flux with remote sensing data. Especially, the development of the quantitative thermal infrared remote sensing strongly attracts many meteorologist and hydrologist. Some quantitative remote sensing scientists have paid much attention to the surface temperature because the information provided by surface temperature is the synthetical result of the heat and water balance in surface. So the information about the heat balance and water balance is implied in the surface radiative temperature. How to extract and excavate the information is a key problem. For about two decades, several remote sensing models and methods were developed to estimate the 2-D distribution of surface flux[1—7]. Generally speaking, at present,

one-layer models for wet dense vegetation mainly include SEBAL[8] and SEBS[9] that is an improved model based on SEBAL. The essential of these models is that the mixed pixel composed of leaf and soil is treated as a big leaf. In their application, wet and dry point are selected in remote sensing image and the experimental relationship between air and surface temperature is used to eliminate the air temperature that is difficult to estimate by means of remote sensing. These models are suitable for the regions with dense vegetation. However, in semi-wet or semi-arid regions without dense vegetation, taking soil and vegetation into account respectively would be more reasonable. Deardorff[10], Dickson[11], Suttleworth[12] et al. proposed the resistance-network concept to separate soil from vegetation. Choudrury and Monteith[13,14] expanded the tow-layer model based on resistance-network. Although a set of equations with six equations and six unknowns are built, the system is still limited in field scale of agriculture meteorology. Norman developed a parallel two-layer model (N95)[15] and proposed the key steps to separate radiative surface temperature with multi-angular infrared measurements. They still used Beer's Law to separate the net radiation. Its essential is to simplify the resistance-network concept of two-layer model. N95 model combined the remote sensing data and the surface data, developed the application of two-layer model in region scale. Then, Kustas et al. made some improvements on the parallel two-layer model and physically explained differences between the parallel model and other models such as the system model, the patch model. They also analyzed the uncertainty on the separation of net radiation with Beer's Law[16–19]. However, they did not discuss the separation method of mixed radiative temperature with multi-angular measurements and its uncertainty in detail.

ATSR sensor, lunched by European Space Agency (ESA), has some special instruments with forward 53° and nadir view angles to gain the thermal infrared images. This sensor provides a new way for separating temperature of soil from that of vegetation[20]. The uncertainty of this method is that the pixel (1.06 km×1.06 km) measured at nadir view angle is not identical with the pixel (2 km×1.5 km) measured at forward view angle. Thus, their areas and shapes are different and the users have to resample the remote sensing images. Because the areas are different between the pixel scaled by some pixels at nadir view and the pixel scaled by some pixels at forward view, some errors are introduced. Furthermore, re-sampling will reduce the spatial resolution of remote sensing data. On the other hand, remote sensing data source used widely now do not provide multi-angular data, which also limits the wide use of this method.

Another temperature separation method of the mixed pixel presented by us before is to utilize the two-temporal data in morning/noon to retrieve thermal inertia information and building another equation to estimate T_v and T_s[21–23]. The advantage of this method is to use thermal infrared multi-temporal information to separate surface temperature with NOAA-AVHRR and MODIS data. The disadvantage lies in the fact that factorial coefficient of the local thermal inertia and wind must be determined by experiment. Based on our original model and research, a new operational two-layer model and its theoretical basis (including PCACA algorithm, theoretical positioning algorithm and two-layer energy-dividing algorithm) are proposed. The physical basis of PCACA algorithm to separate the albedo of mixed pixel and two-layer energy-separation algorithm to separate net radiation of mixed pixel has been discussed. The method and principle of separating radiative temperature and net radiation of mixed pixel has been emphasized. The above methods have been validated by MODIS data and simultaneous measurements in Dongping Lake. The surface flux retrieval steps, including MODIS data receiving, cloud mask, multi-band matching process, atmospheric correction, separation of surface temperature and net radiation, the retrieval steps of surface flux, simultaneous calibration in Dongping Lake, scaling of pixels, validation with data from Yucheng Station, are described.

1 Establishment of the PCACA algorithm

1.1 The physical basis of PCACA and temperature decomposition

T. Carlson met many difficulties in the process of

quantitatively solving the equations with too many unknowns. So in order to satisfy the need for application, the information link between NDVI and pixel radiative temperature was proposed to simply analyze the moisture availability of the surface, then a direct and concise analytical method was found. This method is very valuable in some cases for its simplification[24].

Moran (1989) did a series of experiments in eighteen alfalfa fields with various fractional vegetation cover (VFC) and various water-deficiency. The experiments lasted for more than 90 days, the whole growth period of alfalfa. The results indicated that the surface temperatures for different VFC all fell into a trapezium constructed by the vegetation index and surface temperature. The linear interpolation between wet and dry line of the trapezium, could be used to quantitatively estimate the water deficiency of alfalfa[25,26].

The above studies indicate that abundant information will be explored through combining vegetation index with surface temperature. Here, the information will be used to drive the algorithm for separating temperature of the mixed pixels.

The relationship between the temperature of mixed pixel and VFC can be expressed as

$$\sigma\varepsilon_m T_m^4 = \sigma\varepsilon_v f T_v^4 + \sigma\varepsilon_s (1-f) T_s^4, \quad (1)$$

where T_m, T_v and T_s are respectively the surface temperature of mixed pixel, vegetation canopy and soil surface. ε_m, ε_v and ε_s are the emissivity of mixed pixel, vegetation and soil surface. σ is the Stefan-Boltzmann constant. f is VFC of mixed pixel. T_m, f, ε_v and ε_s in eq. (1) could not be retrieved, because there are two unknowns in one equation. So another equation is needed to solve. One known method is to build two equations with two angular measurements:

$$\sigma\varepsilon_m T_{m1}^4 = \sigma\varepsilon_v f_1 T_{v1}^4 + \sigma\varepsilon_s (1-f_1) T_{s1}^4, \quad (2)$$

$$\sigma\varepsilon_m T_{m2}^4 = \sigma\varepsilon_v f_2 T_{v2}^4 + \sigma\varepsilon_s (1-f_2) T_{s2}^4, \quad (3)$$

where subscripts 1 and 2 represent the two different angles. T_v and T_s could be retrieved using these two equations. T_{v1} and T_{v2} measured under two angles must be identical, So is T_{s1} and T_{s2}. Seen from eq. (1), T_m, the temperature of mixed pixel, could be expressed as the function of T_v , T_s and f. Computing the differential coefficient of T_m, we could get eq. (4):

$$4\varepsilon_m T_m^3 \frac{dT_m}{df} + T_m^4 \frac{d\varepsilon_m}{df} = \varepsilon_v T_v^4 - \varepsilon_s T_s^4. \quad (4)$$

Multiply f on the two sides of eq. (4) and rearrange this equation:

$$f\left(4\varepsilon_m T_m^3 \frac{dT_m}{df} + T_m^4 \frac{d\varepsilon_m}{df}\right) = f\varepsilon_v T_v^4 - f\varepsilon_s T_s^4. \quad (5)$$

Solving eqs. (1) and (5), T_s could be expressed as

$$T_s = \left\{\frac{1}{\varepsilon_s}\left[\left(\varepsilon_m T_m^4 - f\left(T_m^4 \frac{d\varepsilon_m}{df} + 4\varepsilon_m T_m^3 \frac{dT_m}{df}\right)\right]\right\}^{\frac{1}{4}}. \quad (6)$$

Solving eqs. (1) and (4), T_v could be expressed as

$$T_v = \left\{\frac{1}{\varepsilon_v}\left[\left(\varepsilon_m T_m^4 + (1-f)\left(T_m^4 \frac{d\varepsilon_m}{df} + 4\varepsilon_m T_m^3 \frac{dT_m}{df}\right)\right]\right\}^{\frac{1}{4}}, \quad (7)$$

where ε_v can be replaced by the mean value, which will not introduce large errors. f can be measured in experiment. ε_m can be estimated from power-weighted equation. $d\varepsilon_m/df$ can be achieved by means of simulated arithmetic. So the problem of separating mixed pixel's temperature can be solved if dT_m/df is estimated. The above steps can be simplified when the following approximation are introduced.

$$T_m^4 \frac{d\varepsilon_m}{df} \approx 0, \quad \varepsilon_v \approx \varepsilon_s \approx \varepsilon_m. \quad (8)$$

And the above procedures are all based on the assumption that $dT_v/df \approx 0$, $dT_s/df \approx 0$. However, in pixel scale, these two equations are not equal to zero in practice because the humility is always larger and the surface temperature of vegetable canopy is always lower in dense vegetation. Supposing that $2dT_v/df \approx dT_m/df$ and $2dT_s/df \approx dT_m/df$, the expression can be simplified as

$$2\frac{dT_m}{df} \approx (T_v - T_s). \quad (9)$$

The above result indicates that whether for the complete expression of T_m^4 or for the simplified expression of T_m, T_v and T_s all can be calculated. So every pixel's position in the trapezium can be determined according to its T_s–T_v, T_m, and f. Of course, some pixel's positions probably can be overlapped (fig. 1). When VFC of one pixel is determined, a T_m value can be obtained through infinite combinations of T_s and T_v. In addition, because the rate of soil water supply is equal for the same slope line in the trapezium, not only T_s–T_v is equal for the same slope line, but also T_s and T_v are respectively equal and only VFC is variable. Our aim is to separate the surface temperature into T_s and T_v. To do that, the distribution of mixed radiative temperature-VFC for all pixels is analyzed as the following. Its feasibility is also analyzed theoretically.

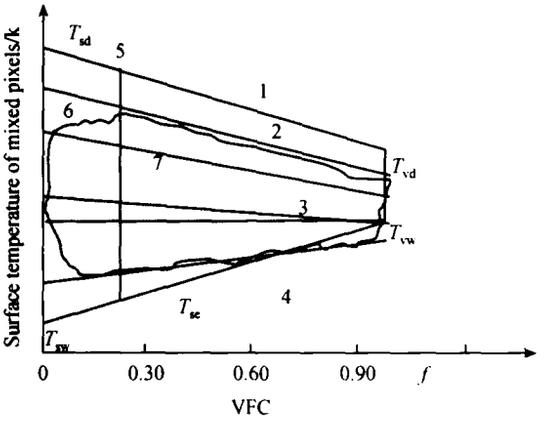

Fig. 1. Trapeziform structure, theoretical position of every kind of lines and points. 1, Absolute dry line; 2, actual dry line; 3, actual wet line; 4, absolute wet line; 5, equal fractional vegetation cover; 6, envelop line of pixels; 7, equal slope.

The essence of the above method is to simulate T_m's variability with f, namely dT_m/df by pixel-arranging method and achieve the solutions with analytic geometry method. The principle of this method is the same as that of the multi-angular method. The multi-angular method is to obtain different VFC and radiative temperature of mixed pixels with equal soil temperatures and equal vegetation temperatures under two different angles. Similarly, the principle of the pixel-arranging method is that isolines exist in the correlative figure of temperature and VFC, with identical soil temperature, vegetation canopy temperature, sensible heat flux, latent heat flux of every pixel, but the radiative temperature is different due to VFC difference for each mixed pixel. So, along an isoline the difference of VFC is similar to the difference caused by two different view angles. And the method overcomes the uncertainty due to the different areas measured in two view angles. This method is called Pixel Component Arranging and Component Algorithm (PCACA).

Supposing that the coupling mechanism between soil and vegetation canopy accords with the two-layer model proposed before[22] and differs from the patch two-layer model and modification was made in the physical concept: the minimum unit of two-layer model is composed of the soil under a single plant and the near soil, then their radiative sources and driving forces can be different. However the surface temperature of soil can be different from surface temperature of canopy. In the minimum unit water resource of vegetable root is the same as that of soil (with root) due to expansion of vegetable root and infiltration of soil water. When the prevailing minimum units are integrated, water sources of bare soil and the soil under vegetation are the same. So some transitional lines exist between the dry line and the wet line and are identical with the slope lines. The above assumptions have been validated by the researches of Moran[25,26].

The uncertainty of these assumptions comes from differences from the patch parallel two-layer model where completely different soil water conditions exist for soil with relatively large area and dense vegetation in one pixel.

1.2 The theoretical positioning and retrieval method of wet line and dry line

According to the above analysis, the key step of separating temperature of mixed pixel is how to calculate dT_m/df. During the calculation, if the extreme dry point, wet point and points with various VFC all exist in the region, which is an ideal condition, the

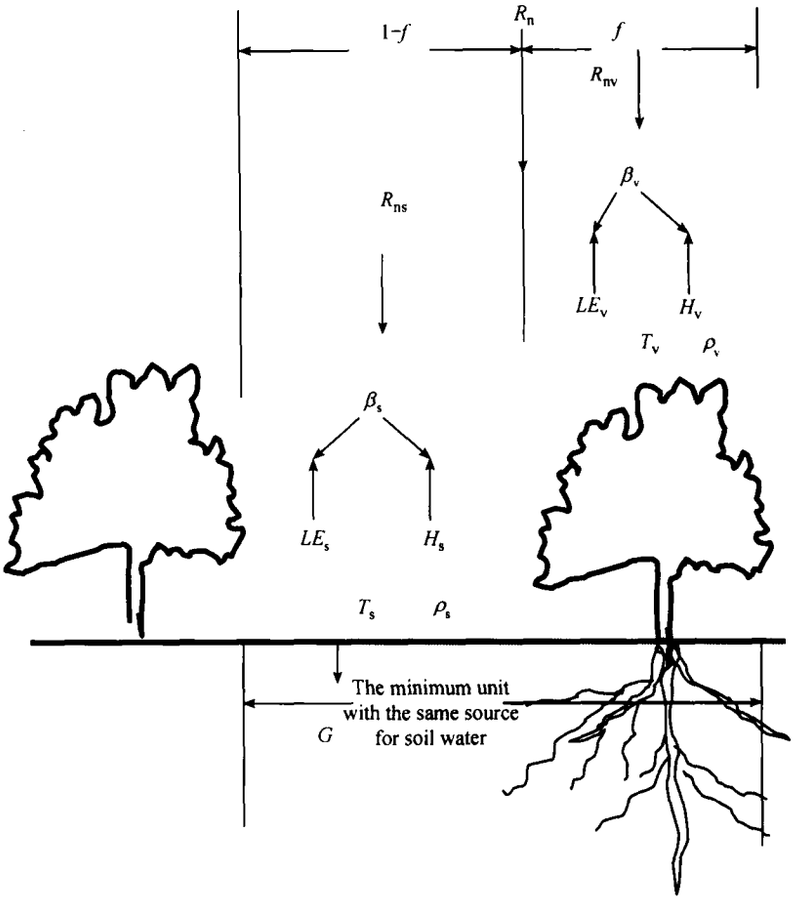

Fig. 2. The minimum unit of two-layer energy balance model with the same source for soil water.

coordinate position of each pixel will be arranged to straight lines and the lines with various slopes will constitute a good shape trapezium. If some points with certain conditions, especially the extreme dry point and wet point do not exist in the research region, these points will not appear in the region where between the dry point and the wet point, even the vacant region will happen. So the line of the trapezium of the pixels will deviate from the dry line and the wet line, and the convex and the concave will happen. That is to say, some points are absent in the trapezium, which will cause the uncertainty in the calculations of dry line, wet line and dT_m/df.

In fact, each component T_m in the trapezium graph is controlled by thermal energy balance equation. When solar radiation, wind speed do not change much in larger region, besides T_m, f, wetness index w is also a chief parameter and the heat energy balance equation can be expressed as

$$R_n - G = H + LE. \tag{10}$$

If soil heat flux G and net radiation R_n has the following relationship $G \approx 0.3(1-0.9f)R_n$, eq. (11) can be obtained:

$$R_n[1-0.3(1-0.9f)] = H + LE. \tag{11}$$

When the soil is very dry, an extreme condition, there is no soil water evaporation, vegetation transpiration, and the soil water is close to the wilting coefficient, the thermal energy balance equation is

$$R_n[1-0.3(1-0.9f)] = H. \tag{12}$$

For dry bare soil, $f = 0$, its thermal balance equation can be written as

$$0.7\left[S_0(1-\alpha_{SD})+\sigma\varepsilon_a T_{sky}^4-\sigma\varepsilon_{SD}T_{SD}^4\right]=\frac{\rho C_p(T_{SD}-T_a)}{r_{SD_a}}. \quad (13)$$

After rearranging the equation, we get

$$\frac{\rho C_p}{r_{SD_a}}T_{SD}+0.7\sigma\varepsilon_{SD}T_{SD}^4 = 0.7[S_0(1-\alpha_{SD})+\sigma\varepsilon_a T_{sky}^4]+\frac{\rho C_p}{r_{SD_a}}T_a, \quad (14)$$

where T_{SD} is the bare soil temperature, ρ is density of air, c_p is the volumetric heat capacity of air, r_a is the air dynamic resistance, ε_{SD} is the emissivity of soil surface, σ is the Stefan-Boltzmann coefficient, S_0 is the solar incident total radiation, α_{SD} is the albedo of dry bare soil, ε_a is the emissivity of air.

An iterative algorithm is used to solve the equation, and T_{SD} can be expressed as

$$T_{SD}=\frac{0.7[S_0(1-\alpha_{SD})+\sigma\varepsilon_a T_{sky}^4]+\frac{\rho C_p}{r_{SD_a}}T_a}{\frac{\rho C_p}{r_{SD_a}}+0.7\sigma\varepsilon_{SD}T_{SD}^3}. \quad (15)$$

If T_{SD}^3 is replaced by T_{ASD}^3, eq. (15) can be simplified as an algebraic equation. T_{SD} can be expressed as

$$T_{SD}=\frac{0.7[S_0(1-\alpha_{SD})+\sigma\varepsilon_a T_{sky}^4]+\frac{\rho C_p}{r_{SD_a}}T_a}{\frac{\rho C_p}{r_{SD_a}}+0.7\sigma\varepsilon_{SD}T_{ASD}^3}. \quad (16)$$

The most parameters on the right side of eq. (16) can be measured in flux observation station or agro-meteorological station, or meteorological station, hydrology station that is just located in or close to the extremely dry bare soil pixel. The best method is to build dry bare soil calibration field and measure these parameters with Large Aperture Scintillometer (LAS). Among these parameters, direct solar radiation, sky equivalent temperature and wind speed can be represented using one point value and can be expanded in the spatial scale. The albedo of dry bare soil is a stable value for certain roughness length and solar zenith angle. The resistance of dry bare soil for some typical surfaces is mainly determined by local wind speed that can be calculated through the wind speed distribution data from county meteorological station network. Therefore, r_{SDa} can be computed. Thus, T_{SD} can be calculated from eq. (16). That is to say, the position of dry bare soil is theoretically determined.

Following the above idea, when VFC is up to 100%, surface temperature becomes canopy surface temperature, and soil water content under the canopy should be the same as water content of the dry bare soil. The parameters like albedo, air dynamic roughness length and vegetation surface temperature are changing. From dry bare soil albedo to dry vegetation albedo along the dry line, T_{VD}, the surface temperature of dry and full cover vegetation, can be expressed as

$$T_{VD}=\frac{0.97[S_0(1-\alpha_{VD})+\sigma\varepsilon_a T_{sky}^4]+\frac{\rho C_p}{r_{VD_a}}T_a}{\frac{\rho C_p}{r_{VD_a}}+0.97\sigma\varepsilon_{VD}T_{AVD}^3}. \quad (17)$$

According to the theoretical analysis, the vegetation at that time is in strong water stress condition. Most of the parameters on the right side of eq. (17) can also be measured in flux observation station or agro-meteorological station, or meteorology station, hydrology station that is just located in or close to the extreme dry bare soil pixel. Building dry bare soil calibration field is the best method, too. The albedo of vegetation is also a stable value for certain roughness length and solar zenith. The resistance of dry vegetation for some typical surfaces is mainly determined by the wind speed and crop height. The local wind speed can be calculated through the wind speed distribution data from county meteorology stations. The crop height can be expressed by the mean height in the region. Based on crop classification, with a remote sensing model for crop height of wheat, cotton and corn proposed by us in Yucheng ecological station, crop height can be retrieved from MODIS data[28].

Therefore, the typical r_{VD_a} of dry vegetation field can be computed. Thus, T_{VD} can be calculated from eq. (17) and its position can be theoretically determined.

When the soil is very humid, namely wet bare soil, another extreme condition appears. There is no sensible heat flux. The energy for the evaporation is (R_n-G) and the thermal energy balance equation can be expressed as

$$R_n(1-0.3)=LE, \tag{18}$$

$$0.7\left[S_0(1-\alpha_{SW})+\sigma\varepsilon_a T_{sky}^4-\sigma\varepsilon_{SW}T_{SW}^4\right] = \frac{\rho C_p \Delta\left(T_{SW}-T_{SW_a}+\frac{d_{SW}}{\Delta}\right)}{\gamma r_{SW_a}}. \tag{19}$$

The temperature of wet bare soil can be expressed as

$$T_{SW}=\frac{0.7\left[S_0(1-\alpha_{SW})+\sigma\varepsilon_a T_{sky}^4\right]+\frac{\rho C_p\Delta}{\gamma r_{SW_a}}\left(T_{SW_a}-\frac{d_{SW}}{\Delta}\right)}{\frac{\rho C_p\Delta}{\gamma r_{SW_a}}+0.7\sigma\varepsilon_{SW}T_{ASW}^3}, \tag{20}$$

where γ is the psychrometric constant, d_{SW} is the air saturation deficiency of wet bare soil, Δ is the slope of the saturation vapor pressure-temperature curve. Local wind speed data can be retrieved through the wind speed distribution data from county meteorology stations. So, the typical r_{SW_a} of wet bare soil can be calculated. Thus, T_{SW}, the third extreme point in the trapezium, can be calculated from eq. (20) and its position can be theoretically determined.

When vegetable cover is up to 100%, the surface temperature is the canopy temperature and the amount of soil water under the canopy should be the same as the wet bare soil. From wet bare soil albedo to wet vegetation albedo along the wet line, T_{VW}, the surface temperature of wet and full cover vegetation, can be expressed as

$$T_{VW}=\frac{0.97[S_0(1-\alpha_{VW})+\sigma\varepsilon_a T_{sky}^4]+\frac{\rho C_p\Delta}{\gamma r_{VW_a}}\left(T_{VW_a}-\frac{d_{VW}}{\Delta}\right)}{\frac{\rho C_p\Delta}{\gamma r_{VW_a}}+0.97\sigma\varepsilon_{VW}T_{AVW}^3}, \tag{21}$$

where d_{VW} is the aerial saturation deficiency of wet and full cover vegetation. According to the theoretical analysis, the vegetation at that time is in the completely humid condition. The resistance of wet vegetation, r_{VWa}, is mainly determined by wind speed and vegetation height under some typical surfaces. Local wind speed data can be retrieved through the wind speed distribution data from county meteorology stations. Vegetation height can be expressed by the mean height in the region. So, the typical r_{VWa} of wet and full cover vegetation can be calculated.

Finally, the coordinate of wet vegetation field in the trapezium was determined in theory (fig. 1). After the four extremums of surface temperature were all determined, the coordinates of dry line and wet line were also found. Thus, PCACA could be improved in some degree. The solution of above equations was obtained through an approximate algorithm that was directly calculating the four angles T_m of the trapezium from the four equations. This arithmetic was feasible, which could be confirmed by the similar result of Moran[25,26]. Of course, it should be indicated that calculating the four values still needs some parameters like air resistance, but this arithmetic had cut down these parameters from all pixels to only four pixels. They can be achieved by the observations in the calibration field. So development from un-operational algorithms to an operational one is a large advance.

After the frame of the trapezium was determined, dT_m/df of all pixels between the dry line and the wet line could be achieved through computing the slopes.

1.3 Separating albedo of mixed pixels by PCACA

After obtaining the net radiation by remote sensing, Beer's Law was adopted in many two-layer models to separate net radiation of mixed pixel. This idea has some uncertainties according to further practices. Beer's Law quantitatively describes the radiative attenuation process when radiation passes through the medium. When radiation passes through vegetation canopy, the attenuation is a negative exponent function parameterized by the geometrical structure of vegetation and leaf area index. The separation of mixed net radiation through Beer's Law, in fact, is determining

the proportion of the gap and the non-gap by the parameters like LAI, leaf angle and assigning mixed net radiation between vegetation and soil. If differences between albedo of vegetation and that of soil are small, the error is small too. Conversely, if differences are large, the error is large. In practice, sometimes, the difference of albedo and surface temperature between vegetation and soil is very large. In many cases, soil's temperature can be more than 10℃ than vegetation's. Therefore, it is more reasonable to calculate the net radiation of vegetation and soil, respectively.

Net radiation is composed of short wave net radiation in visible and nadir band and long wave net radiation in thermal-infrared band. So, in order to achieve it, besides the separation of radiometric temperature of mixed pixel, albedo of mixed pixel must be separated. The albedo of soil mainly depends on soil wetness, soil type, soil roughness length, etc. Its range is larger. Vegetation albedo mainly depends on leaf color, canopy structure, etc. Its range is small. Because the purpose of getting albedo is to calculate net radiation, only the integral value of every influencing factor needs to be considered. Albedo of mixed pixel is the weighed-average value of the soil's and vegetation's integral. The envelope line of the albedo-VFC correlative figure shows trapeziform shape, which is more standard than the shape of temperature-VFC correlative figure. So PCACA can also be applied to separating albedo of the mixed pixels. Equations on albedo and VFC are as follows:

$$\alpha_m = (1-f)\alpha_s + f\alpha_v, \tag{22}$$

$$\frac{d\alpha_m}{df} = \alpha_v - \alpha_s, \tag{23}$$

$$\alpha_s = \alpha_m - f\frac{d\alpha_m}{df}, \tag{24}$$

$$\alpha_v = \alpha_m + (1-f)\frac{d\alpha_m}{df}, \tag{25}$$

where α_s, α_v and α_m respectively is the average albedo of soil, vegetation and mixed pixel. α_s and α_v of every pixel can be achieved through eqs. (24), (25). It is obvious that α_s and α_v depend on albedo of the mixed pixel and the differential coefficient of albedo to VFC. The former is a known number, so the key problem is how to get the latter. Same as the separation of radiometric temperature, this derivation is the slope of the mixed albedo-VFC line and can be achieved by PCACA. It should be noticed that soil temperature is generally higher than canopy temperature, so the slope of should be negative in most cases. However, because of soil wetness's effects on soil albedo, the slope is either negative or positive. When $\alpha_s > \alpha_v$ (for the full bands), the slope is negative. On the contrary, the slope is positive.

In practice, provided that soil type and soil roughness length are the constant, soil albedo mainly depends on soil wetness. Between up-envelop line and down-envelop line, there are transitional soil wetness isolines. That is to say, slope isolines and wetness isolines are the same line.

2 Layered energy-separating algorithm of Bowen Ratio and its theoretical basis

Above study has pointed out that the originality of many two-layer models is built on the basis of soil-vegetation resistance network. The computation of complicated resistance network needs many factors, such as surface roughness length, local wind speed, atmospheric stability, friction velocity, Monin-Obukhov length, boundary layer height, etc. The more complicated the model is, the more difficult the retrieval is in regional scale. Thus, the retrieval just can be done in field microclimate scale.

Provided that there is no advection, it can easily get sensible heat flux and latent heat flux using Bowen Ratio to separate available energy (net radiation-soil heat flux). This simple method avoids air temperature and various surface resistances. They cannot be achieved directly by remote sensing.

There are three key factors determining Bowen Ratio defined as sensible heat flux divided by latent heat flux. They are soil water content, differences between heat and vapor turbulent transport and differences between dry and wet air molecular diffusion. Among the three factors, the soil water content is the

most important because it determines the rate of soil water supply. The other two factors are subordinate, which can be expressed by psychrometric constant γ and the slope of the saturation vapor pressure-temperature curve Δ. Bowen Ratio of vapor saturated land surface or water surface is the smallest.

The relationship between Bowen Ratio and the rate of soil water supply is the theoretical basis of this kind of method that separating energy. There is an explicit functional relationship between the rate of soil water supply M and latent heat flux LE. When M is a constant and combines with crop water stress index F[3] and Bowen Ratio $\beta = H/LE$, where H is the sensible heat flux, LE is the latent heat flux, the relationship of M, F, β is the following:

$$1-F=M=\frac{LE}{LE_0}=\frac{H}{\beta LE_0},$$
$$\beta=\frac{H}{MLE_0}. \tag{26}$$

Eq. (26) shows the precise and simple physical relationship among the rate of soil water supply, crop water stress index and Bowen Ratio. The key equation is the function of M and β which can be achieved through PCACA.

$$M_i \approx \frac{T_{mH}-T_{mi}}{T_{mH}-T_{mL}}=\frac{LE_i}{LE_0}, \tag{27}$$

$$\beta_{mi} \approx \frac{T_{mH}-T_{mL}}{T_{mH}-T_{mi}}-1, \tag{28}$$

where T_{mi} is the true temperature of i pixel (similar to radiometric temperature) in a certain VFC, T_{mH} and T_{mL} respectively are the true temperature of i pixel on the dry line and on the wet line in the same VFC. Can the two-layer model use this algorithm? The following is the answer. The vegetative latent heat flux can be achieved only by Priestley-Taylor approximation[27] in N95 model[15].

$$LE_v = af\frac{\Delta}{\Delta+\gamma}R_{nv}, \tag{29}$$

where R_{nv} is the vegetative net radiation, a is the experimental coefficient. Through many years' experiments, Priestley-Taylor indicated that the average of a is 1.26[27]. On the canopy surface, Norman adopts a = 1.3. For the maize and cotton canopy, Kustas adopts a = 2.0. f is VFC whose expression is the same as Priestley-Taylor's. In N95 model, the vapor on the green vegetation was regarded as almost saturation, which is an approximate method. The function of β, Δ and γ can be expressed as

$$(R_n-G)=(1+\beta)LE,$$
$$\beta=\frac{\Delta+\gamma-a\Delta}{a\Delta}. \tag{30}$$

In eq. (29), $af[\Delta/(\Delta+\gamma)]$ is similar to β. In fact, layered energy-separating algorithm has been adopted in N95 model. According to the above analysis, layered energy- separating algorithm has theoretical and practice basis. To the further development, after soil net radiation and vegetative net radiation are obtained, soil Bowen Ratio β_{si} and vegetative Bowen Ratio β_{vi} can be obtained too using the layered energy- separating algorithm. So soil sensible/latent heat flux and vegetation sensible/latent heat flux can be achieved. Finally, construct correlative figure of soil surface temperature-VFC, correlative figure of canopy temperature-VFC and achieve the trapezium by eqs. (17), (19), (20) and (21). And then β_{si} and β_{vi} can be obtained by the following equations:

$$\beta_{Si} \approx \frac{T_{SH}-T_{SL}}{T_{SH}-T_{Si}}-1, \tag{31a}$$

$$\beta_{Vi} \approx \frac{T_{VH}-T_{VL}}{T_{VH}-T_{Vi}}-1. \tag{31b}$$

The uncertainty of this method mainly results from ignoring advection. $LE_0 = R_n-G$ is reasonable only when there is no advection, that is to say, the energy of subtracting soil heat flux from net radiation is all used for evapotranspiration. Namely, the evapotranspiration is equal to the maximum evapotranspiration. However, when there is advection the above energy balance equation is untenable. The external energy AD must be considered and $R_n-G + AD = LE + H$. From the scaling transform, for MODIS

data and NOAA data whose resolution is 1.1 km in thermal-infrared band, the advection's effects on the net radiation in this pixel scale still need further re-consideration. Under the optimistic point of view, because of the effects of advection, the fetch is about 200 m when the instrument is 2 m high. According to its regular, it only has effects on the edge of the pixel and the advection effects caused by surface's heterogeneous inside the pixels are eliminated by pixels' average action. Of course, it is an important work about scale transformation of surface flux.

3 Other keys about retrieval of the two-layer model

3.1 The inversion and decomposition of the true surface temperature of mixed pixel

Although ready-made land surface temperature (LST) product is available, radiative correction must be performed by MODTRAN4.0 or split-window arithmetic when the difference between product LST and measured LST on Dongping Lake point is large. The following is the method of retrieving true surface temperature.

Surface radiative temperature observed on the top of the atmosphere by MODIS results from atmospheric upward thermal radiance, reflectance of atmospheric downward thermal radiance. According to eq. (32), in order to get every pixel's true surface temperature T_{0i}, every pixel's radiative temperature, emissivity ε_i and equivalent sky temperature T_{sky} must be known.

$$T_{0i} = \left[\frac{T_{mi}^n - (1-\varepsilon_i)T_{sky}^n}{\varepsilon_i}\right]^{\frac{1}{n}}, \tag{32}$$

where n is determined by band, for example, n = 4 from 8 μm to 14 μm. Emissivity of mixed pixel ε_i is expressed as

$$\varepsilon_{mi} = f\varepsilon_{vi} + (1-f)\varepsilon_{gi} + \Delta\varepsilon, \tag{33}$$

$$\varepsilon_{dgi} = \varepsilon_{wgi} - \frac{T_{mi} - T_{dmai}}{T_{dmpi} - T_{dmai}} \times 0.06,$$

where ε_{mi}, ε_{dgi}, ε_{wgi}, ε_{vi} are mixed pixel, dry soil, wet soil and vegetation canopy emissivity, respectively. $\Delta\varepsilon$ is the complement caused by the discrepancy of soil, vegetation temperature and their emissivity. $(T_{mi} - T_{dmai})/(T_{dmpi} - T_{dmai})$ is relative thermal inertia, where T_{dmpi} and T_{dmai} respectively are the radiative temperature of the dry soil whose emissivity is 0.89 at noon and at early morning. So, in the process of computing emissivity, not only is VFC considered, but also soil water content is considered, which improved the accuracy and the rationality of the computing. According to the long measurement in Yucheng remote sensing experiment field, dry soil's emissivity is 0.89, with average surface roughness length. It increases with the increase of soil water content and the rate of change is determined by this equation $0.06(T_{mi} - T_{dmai})/(T_{dmpi} - T_{dmai})$. The emissivity of most wet soil can reach 0.95. The average vegetation emissivity is 0.98.

The average atmospheric downward thermal radiance can be expressed by the surrounding vapor pressure e_a and air temperature T_a.

$$T_{sky} = (1.24e_a^{0.14}T_a^{3.86})^{0.25}. \tag{34}$$

The observer can see the sky only about 25 km diameter because of the effect of the earth curvature. Therefore, the same T_{sky} value can be adopted in the range of 25 km×25 km as the same area as a county. Air temperature data and air vapor pressure data of county weather station are available.

Every pixel's VFC still need to be known when PCACA is used to separate true surface temperature of mixed pixel. The algorithm is as the following[28]:

$$f_i = \frac{NDVI_i - NDVI_g}{NDVI_v - NDVI_g}, \tag{35a}$$

where NDVI, $NDVI_v$ and $NDVI_i$ are the Normalized Difference Vegetation Index of pure soil pixel (VFC is 0%), pure vegetation pixel (VFC is 100%) and mixed pixel, respectively. The referenced values are: NDVI = 0.77 when VFC is 100%, and NDVI = 0.099 when VFC is 0%. If the maximal NDVI is greater than 0.77 and the minimal NDVI is less than 0.099, there is no need to correct f. Otherwise, f needs to be corrected.

The algorithm is the following: provided that the maximal NDVI is A and the minimal NDVI is B, then maximal f (minimal f) corresponding to the corrected maximal NDVI (minimal NDVI) is expressed as $f_{max}(f_{min})$ = (A(or B) − 0.099)/(0.77 − 0.099). So $f_{ri} = f_{min} + f_{oi}(f_{max} - f_{min}) \times f_{min}$, where f_{oi} is uncorrected value, f_{ri} is corrected value. The method is a simple linear interpolation.

After the acquirement of mixed temperature and VFC, the slope of temperature-VFC line and the differential coefficient can be calculated by using PCACA. Then, the regional distribution of T_{si} and T_{vi} can be obtained through eqs. (6) and (7).

Leaf area index (LAI) and VFC are the key parameters in the inversion of crop height. According to Beer's Law and NDVI, LAI can be expressed as[28]

$$\mathrm{LAI} = \ln\left[\left(1 - \frac{\mathrm{NDVI}}{A}\right)B^{-1}\right]C^{-1}, \qquad (35b)$$

where A, B, C are three constants determined by vegetation structure, especially C that has a close relation with leaf angle distribution function and plant overlap function.

3.2 The acquirement and the separation of mixed net radiation

The calculation of net radiation needs the data in visible band, near-infrared band, and thermal-infrared band. When the surface reflectance of atmospheric downward thermal radiance and soil-air multiple reflectance are ignored, every mixed pixel's net radiation is expressed as

$$R_{nmi} = (S_{0i} + D)(1 - \alpha_{mi}) - \sigma\varepsilon_{mi}T_{mi}^4 + \sigma\varepsilon_{sky}T_{sky}^4, \quad (36)$$

where R_{nmi}, S_{0i}, α_{mi}, ε_{mi} and T_{mi} are net radiation, direct solar radiation, surface reflectivity, surface emissivity and surface radiative temperature of i pixel, respectively; D is the down-diffusion radiation in visible and near-infrared band; ε_{sky} and T_{sky} are the atmospheric emissivity and sky equivalent temperature. They have no pixel subscript because they have better representation in large scale; S_{0i} should be corrected by the following equation[28]:

$$\Delta S_{0\varphi} = S_o(\cos\varphi\sin\delta - \sin\varphi\cos\delta\cos\omega)\Delta\varphi, \quad (37a)$$

$$\Delta S_{0\omega} = -S_o\cos\varphi\cos\delta\sin\omega\Delta\omega, \qquad (37b)$$

where S_0 is the direct solar radiation observed in the weather station (like Yucheng Station); $\Delta\varphi$, $\Delta\omega$, $\Delta S_{0\varphi}$ and $\Delta S_{0\omega}$ are the difference between the pixel's latitude and the station's, the difference between the pixel's solar time angle and the station's, the difference of direct solar radiation caused by different latitudes, the difference of direct solar radiation caused by solar time angle, respectively.

The uncertainty of separating net radiation by means of Beer's Law has been analyzed above. In this paper, α_{si}, α_{vi}, T_{si} and T_{vi} can be achieved by PCACA, so net radiation of soil (vegetation) can be expressed as

$$R_{nsi} = [(S_{0i} + D)(1 - \alpha_{si}) - \sigma\varepsilon_{si}T_{si}^4 + \sigma\varepsilon_{sky}T_{sky}^4](1 - f), \quad (38)$$

$$R_{nvi} = [(S_{0i} + D)(1 - \alpha_{vi}) - \sigma\varepsilon_{vi}T_{vi}^4 + \sigma\varepsilon_{sky}T_{sky}^4]f. \quad (39)$$

3.3 The retrieval of layered Bowen Ratio and layered surface fluxes

Soil Bowen Ratio and vegetation Bowen Ratio of pixel i can be obtained through eqs. (31a) and (31b). In the above section, the importance of the four extrema's theoretical locations has been indicated. On the basis of the four extrema, the dry line, the wet line and the frame of trapezium under that weather condition can be obtained. The keys of this step lie in the determination of the dry line's location and the wet line's and whether the following two given conditions are satisfied. One is that there is an linear relationship between the surface temperature of mixed pixel and VFC, which can assure the crop water stress index line (soil water supply line) or equivalent slope line a straight line and has been supplied by Kimes's directional infrared temperature data[29]. The other is that there is a linear relationship between the soil evaporation and the vegetation transpiration with surface temperature. Carlson objectively appraised this hypothesis that it was not complete but feasible[24].

After the layered net radiation and the layered Bowen Ratio of i pixel has been gotten, the following surface flux can be retrieved:

(1) The retrieval of the soil evaporation LE_{si} and the soil sensible heat flux H_{si}

$$LE_{si} = \frac{R_{nsi} - G_i}{1 + \beta_{si}}, \tag{40}$$

$$H_{si} = (R_{nsi} - G_i) - \frac{R_{nsi} - G_i}{1 + \beta_{si}} = \frac{(R_{nsi} - G_i)\beta_{si}}{1 + \beta_{si}}. \tag{41}$$

(2) The retrieval of the vegetation transpiration LE_{vi} and the vegetation heat flux H_{vi}

$$LE_{vi} = \frac{R_{nvi}}{1 + \beta_{vi}}, \tag{42}$$

$$H_{vi} = R_{nvi} - \frac{R_{nvi}}{1 + \beta_{vi}} = \frac{R_{nvi}\beta_{vi}}{1 + \beta_{vi}}. \tag{43}$$

(3) The retrieval of the plant water stress index PWSI

$$\mathrm{PWSI}_i = 1 - \frac{LE_{mi}}{LE_0} \approx 1 - \frac{LE_{mi}}{R_{mni} - G_i}, \tag{44}$$

where LE_{mi} and LE_0 are the true evapotranspiration and the potential (maximum) evapotranspiration of i pixel.

(4) The retrieval of the soil water effective usage rate ζ

$$\zeta_i = \frac{LE_{vi}}{LE_i} \approx \frac{LE_{mi} - LE_{si}}{LE_{mi}}, \tag{45}$$

where LE_{si} and LE_{vi} are the soil evaporation and the vegetation transpiration of i pixel.

(5) The retrieval of the vegetation canopy CO_2 flux $\varphi_{CO_2 i}$

$$\varphi_{CO_2 i} = K\frac{E_{vi}}{D_i}\mathrm{LAI}_i^n \tag{46}$$

where E_v is the transpiration rate whose dimension is mg $\cdot$ s^{-1} $\cdot$ m^{-2} as the same as φ_{CO_2}, not w $\cdot$ m^{-2}; D_i is aerial saturation deficiency on the top of vegetation canopy; K/D_i has no dimension; K = 1/58, n = 1.2; LAI_i is every pixel's leaf area index. If D_i has the following relationship with plant water stress index PWSI, the distribution image of D_i can be obtained.

$$\frac{D_j}{\mathrm{PWSI}_j} = \frac{D_i}{\mathrm{PWSI}_i}, \tag{47}$$

where PWSI_j and D_j is the observed data in weather or ecological station. This method has a stronger physical basis than spatial interpolation algorithm.

4 Experimental results and algorithmic validation

4.1 Surface observation and satellite data's process

According to the PCACA, under the ideal conditions, four calibration fields are needed to determine the four extreme locations. They are dry bare soil field, wet bare soil field, dry full cover field and wet full cover field, respectively. The area of every field should be at least the same as one or two pixels' area. In order to use labor and material resources rationally, two dry fields often can be combined together, as well as the wet fields. That is to say, the dry bare soil field and the dry full cover field are combined into one field; the wet bare soil field and the wet full cover field are combined into one field. Although the calibration fields of pixel scale are quite needed for basic research or for applied science, the investment is very large and the period from establishment to use is very long. Therefore, in order to validate this new algorithm in time, we adopted some data from Dongping Lake field, Yucheng Station and county weather station.

The observation field of the Dongping Lake is located in the Dongping Lake of Shandong Province. Since October 2000, we began to make fixed persons do the observation there. Observation is done when the satellites of NOAA-AVHRR and MODIS passes through. The observer pulls a non-powerboat from the bank to the center and when the boat arrives at the center, it is the time that satellite is passing through. The observation is done during the whole way for about 30 minutes. This method of observation not only can satisfy the need for loop monitoring, but also can eliminate the errors caused by the increase or the de-

crease of the surface temperature and the errors caused by the surface temperature's difference near the bank and in the center. Air temperature, air humidity, wind speed, net radiation at 1.5 m high from water surface and water surface temperature are observed. They are used as referenced data in completely saturated point. Water surface temperature is used to correct the satellite retrieval value.

Yucheng Station is located in Yucheng County of Shandong Province. It has been built for more than 20 years and is an important member of the Chinese ecology network, Chinese Academic Sciences. There are more than 10 experimental fields for different tasks. Among them, the area of remote sensing experimental field is smaller and cannot reach the area of one MODIS pixel. Thus, the measured data only are a reference. In unavoidable cases, the measured temperature can be carefully used to calibrate temperature of soil (vegetation). Measured surface flux data can also be carefully used to validate the retrieval result of the surface flux.

There is a weather station in every county. In these weather stations, observed wind speed at 10 m high, air temperature and air humidity at 2 m can all be used as references. After the pixels of the four extrema are determined, the nearest county weather stations are found according to the latitude and longitude of the four pixels. Using the observed data in these weather stations to calculate the four extreme temperatures, we obtained the frame of trapezium.

Although there is land surface temperature (LST) product in the series of NASA's MODIS products, some LST data are quite different from the observed data in the Dongping Lake. Therefore, we have to retrieve LST by ourselves. After getting the MODIS image data, we used MODTRAN 4.0 to do radiative correction on the basis of which we do geometric correction and multi-band geographic position matching. When thermal inertia information is needed, the process of multi-temporal images geographic position matching becomes very important. In addition, we eliminated the pixels covered by cloud in visible band and near-infrared band. Some other image-processing technologies like selecting study area are not discussed here.

In the process of calculation, we used several computers to operate. So we can divide the work and carry out the computation at the same time. The work platform is ENVI4.0 on the basis of which some new calculating algorithms were developed. Using these algorithms and the models above, we can calculate every pixel's correlative parameters and surface flux frequently and conveniently.

4.2 Results and validation

This paper aims to develop a new and operable PCACA and a layered energy-separating algorithm on the basis of our former two-layer remote sensing model for surface fluxes. The results in this section will validate the physical basis of these two algorithms, the feasibility of retrieving surface flux with limited MODIS data and the precision of the retrieval, which is a methodology research. Although we had observed the surface flux in North China for a long time, we only showed the retrieved results for a certain day due to the space and the limited purpose of this paper. The long-term measured results of the surface flux and its rule will be analyzed in another paper.

Figure 3 is a synthetic true color image of three bands on March 19, 2002, ranging from 110°6′E,

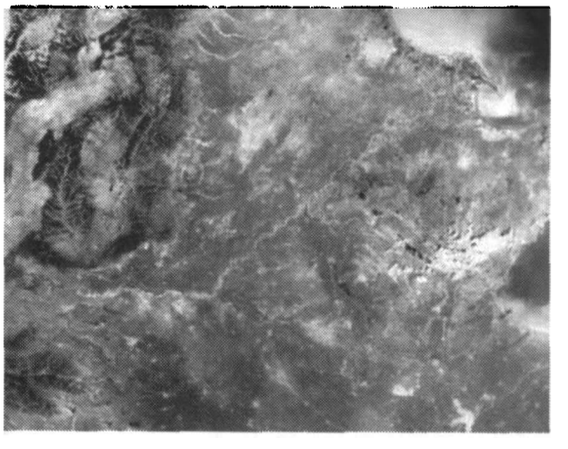

Fig. 3. A synthetic true color image of the experimental area in North China. Time: March 19, 2002. The northeast is Bohai Sea, and the Yellow River can be seen. The northwest is a mountainous area. The majority of area is farmland. Longitude: 110°6′E to 120°14′E, latitude: 33°3′N to 38°38′N.

33°3′N to 120°14′E, 38°38′N. The image covers the most provinces in North China, including a part of the Bohai Sea, the Dongping Lake, Yucheng Station and Beijing. The northwest part in the image is a mountainous area.

Figure 4 shows the correlative scatter figure of the albedo and the VFC. Generally, the envelop line shows a trapeziform shape. The missing points at high VFC show the discontinuous distribution of the albedo. The up-envelop line represents the pixels with high albedo and the low-envelop line represents ones with low albedo. The left up-envelop line is a curve with peak values on which the albedo increases and then decreases with the increase of the VFC. This is an important phenomenon and shows the changing process of the weighted average value between the soil albedo and the vegetation albedo. The left side of the peak value is controlled by soil; the right side of the peak value is controlled by vegetation, and the peak value is the balanced point. According to the above discussion, the albedo follows the radiative balance rule. The up-envelop line and the low-envelop line are the base lines for separating the albedo of mixed pixel. According to the two base lines, the slopes of albedo-VFC lines can be determined. Then, the distribution images of the soil albedo and the vegetation albedo can be retrieved according to eqs. (24) and (25). The two images are not shown here due to the limited space of the paper.

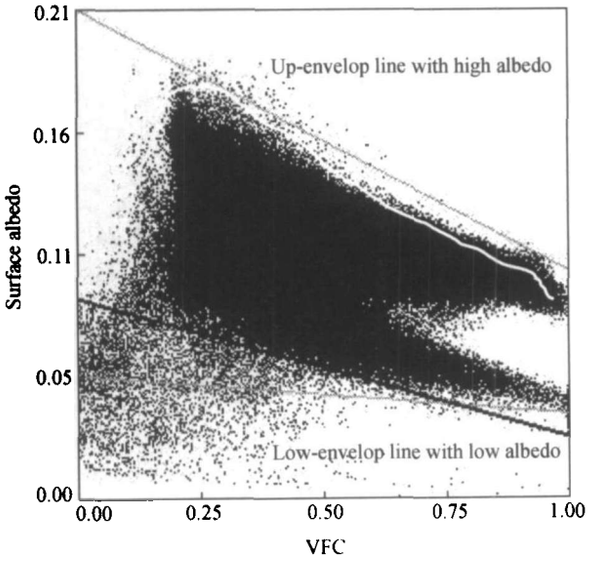

Fig. 4. The correlative scatter figure of the surface albedo and the VFC.

It should be emphasized that thermal infrared surface temperature is the synthetic result of the surface energy balance controlled by net radiation flux, soil heat flux, sensible heat flux and latent heat flux. So the temperature is difficult but necessary to be measured and the correlative scatter figure of the temperature-VFC is the key problem of PCACA. Through correcting and calibrating the thermal infrared images downloaded from the MODIS website, the radiative surface temperature was retrieved, and then in combination with the surface emissivity data and the atmospheric downward thermal radiance data, true land surface temperature is obtained from eqs. (32), (33) and (34). In the whole process, the distribution images of radiative temperature, emissivity, early morning-noon temperature difference and atmospheric downward thermal radiance are retrieved.

NDVI was computed from the visible and near infrared data of MODIS. And then VFC was computed according to eq. (36).The correlative scatter figure of mixed temperature and VFC was done using ENVI.

Actual dry line AB and wet line CD are drawn in fig. 5, which are up-envelop line and low-envelop line, respectively. In the up-envelop line with low VFC, some pixels miss out, where is the bare soil or the field with sparse vegetation. The temperature there is over 295 K. At the places with the same VFC and the temperature lower than 295 K, the pixels are sparse, where are wetlands, waters or sandy beach probably.

The low-envelop line is straighter, presenting a positive gradient. It indicates that in these pixels the soil temperature is lower than the vegetation canopy temperature. This always happens in wetlands, water bodies (lakes, rivers) and sandy beach.

To improve the precision of PCACA algorithm, determining the locations of absolute dry line A′B′ and absolute wet line C′D′ is the key step. That is to say, T_{SD}, T_{SW}, T_{VD} and T_{VW} are calculated according to

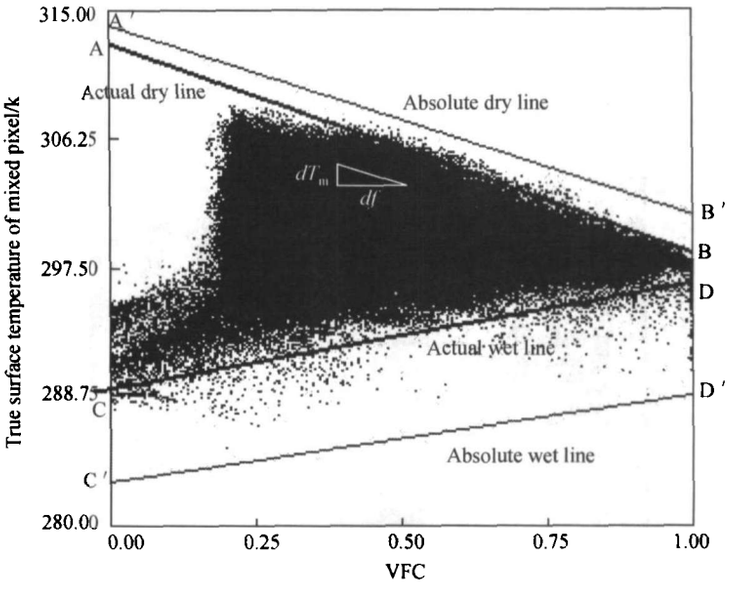

Fig. 5. The scatter figure of true land surface temperature-VFC of mixed pixels.

eqs. (16), (17), (20) and (21). Just as stated above, the temperatures of the four extreme points should be observed and calculated in calibration fields. However, at present we have no such calibration fields, so we utilize the observed data from meteorology stations and ecology stations. The specific steps can be summered as follows: first, to find out the driest bare pixel, the driest full cover pixel, the wettest bare pixel and the wettest full cover pixel on the actual dry line and the actual wet line in the scatter figure. Second, to determine the longitude and the latitude of the four pixels, and find out the county meteorology stations or ecology stations closest to the four pixels, and then, use the observed data of wind speed, air temperature, and air humidity from those stations and MODIS satellite data and eqs. (35a) and (35b) to calculate the distribution images of VFC and leaf area index. Third, to determine the leaf area index of the four pixels and calculate the roughness length and aerodynamic resistance. Finally, we can obtain T_{SD}, T_{SW}, T_{VD} and T_{VW}.

After the positions of the absolute dry line and wet line are determined, the slope of each pixel can be calculated according to the linear interpolation. Then the slope is brought into eq. (9), and together with eq. (1), the true soil surface temperature and the vegetation canopy temperature of each pixel can be solved out; that is, the regional distribution images of the two temperatures can be drawn out. In this way, the PCACA work is finished.

The observed data of solar incident radiation in Yucheng Station and eqs. (37a) and (37b) expressing the solar incident radiation varying with the solar time angle can be used to calculate the distribution image of the solar incident radiation. Combining these data including the images of the soil surface albedo and the vegetation canopy albedo, the distribution images of the true soil surface temperature and the true vegetation canopy temperature, the atmospheric downward thermal radiation and putting them to eqs. (38) and (39), it is then possible to draw the distribution image of the soil net radiation flux and the vegetation net radiation flux. Because of the limited space of this paper, the two images are not shown in this paper.

Figure 6 is the scatter figure drawn from the two distribution images of vegetation canopy surface temperature and VFC. Fig. 7 is the correlative scatter figure of soil surface temperature and VFC. On the basis of the two figures, using the layered energy-separating algorithm, similar to the PCACA algorithm, the absolute dry line and the absolute wet line were drawn out.

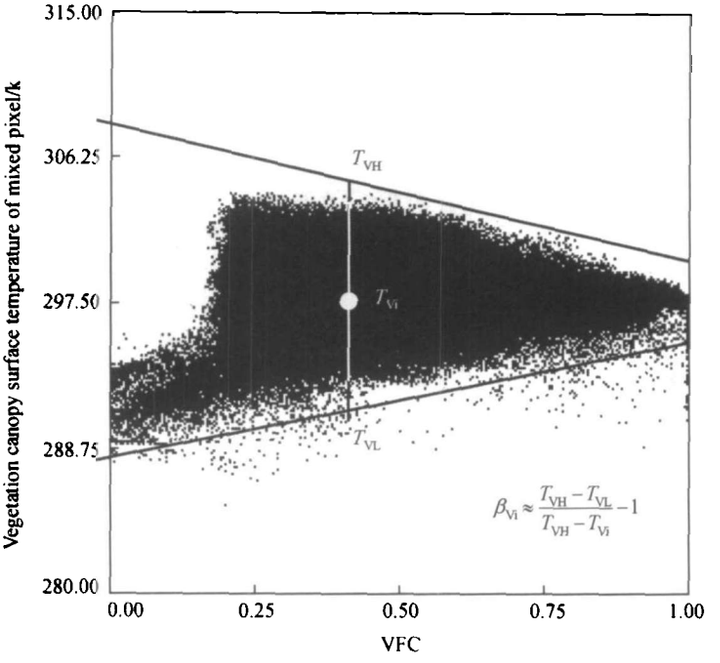

Fig. 6. The scatter figure of vegetation canopy temperature-VFC of mixed pixel.

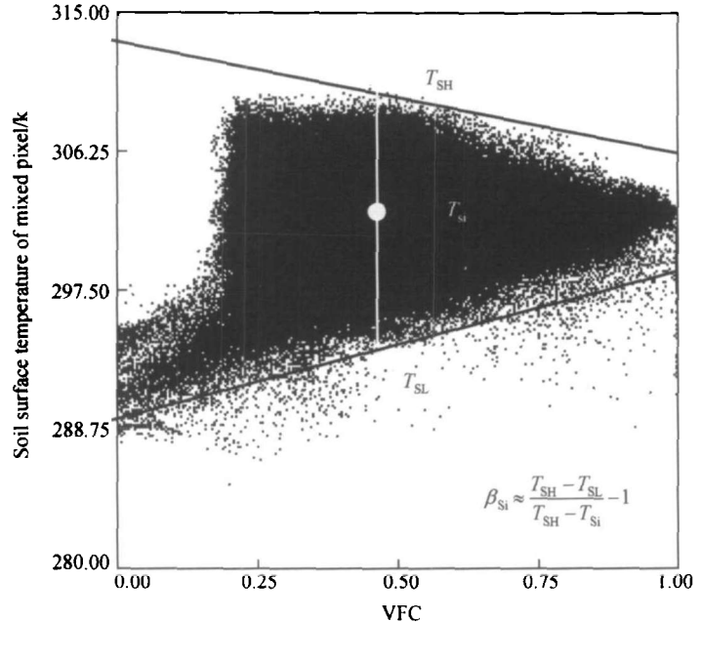

Fig. 7. The scatter figure of soil temperature-VFC of mixed pixel.

Then according to eqs. (31a) and (31b), the Bowen Ratio of the soil layer and the vegetation layer of each pixel could be calculated out, respectively. Together with the distribution images of the net radiation flux of the soil and the vegetation canopy layer, the distribution images of the soil evaporation and the vegetation transpiration could be obtained. The two images are not shown in this paper.

The regional distribution image of the assimilation flux of the vegetation carbon dioxide is the comprehensive result from the all distribution images retrieved above. The validation for the feasibility, reasonableness and the precision of the images is the key problem. According to the key retrieval result, the feasibility, rationality and the retrieval precision of PCACA algorithm and layered energy-separating algorithm are determined too. Therefore, based on eq. (46) and the distribution images of the vegetation canopy transpiration, leaf area index and the air saturation deficiency, the distribution image of the assimilation flux of the vegetation carbon dioxide is drawn out. The distribution image of air saturation deficiency was retrieved according to eq. (47) using the distribution image of the plant water stress index PWSI and air saturation deficiency D in Yucheng station.

Through validating the algorithm from the two aspects, which are the order of magnitudes and the regional distributional characteristics of the retrieved assimilation flux of vegetation carbon dioxide, the retrieved order of magnitudes is reasonable generally. The eddy-correlative observation data in Yucheng station indicated that, in late March, at the moment that MODIS satellites passed through, the assimilation flux of carbon dioxide was no more than 0.3 $mg \cdot s^{-1} \cdot m^{-2}$. The white patches in the distribution image were the farms where the wheat is in good growth, whose order of magnitude is 0.17—0.25 $mg \cdot s^{-1} \cdot m^{-2}$. For example, the high assimilation flux of the carbon dioxide in Jining district, Shandong Province, can be shown reasonably. In mountainous areas, distribution characteristics of the low carbon dioxide assimilation flux in the seashore area of the Bohai Sea and areas of Mount Tai can also be shown reasonably (fig. 8).

Compared with the model we proposed previously, the distinction between the two algorithm is that, in the previous model, the temperature of the mixed

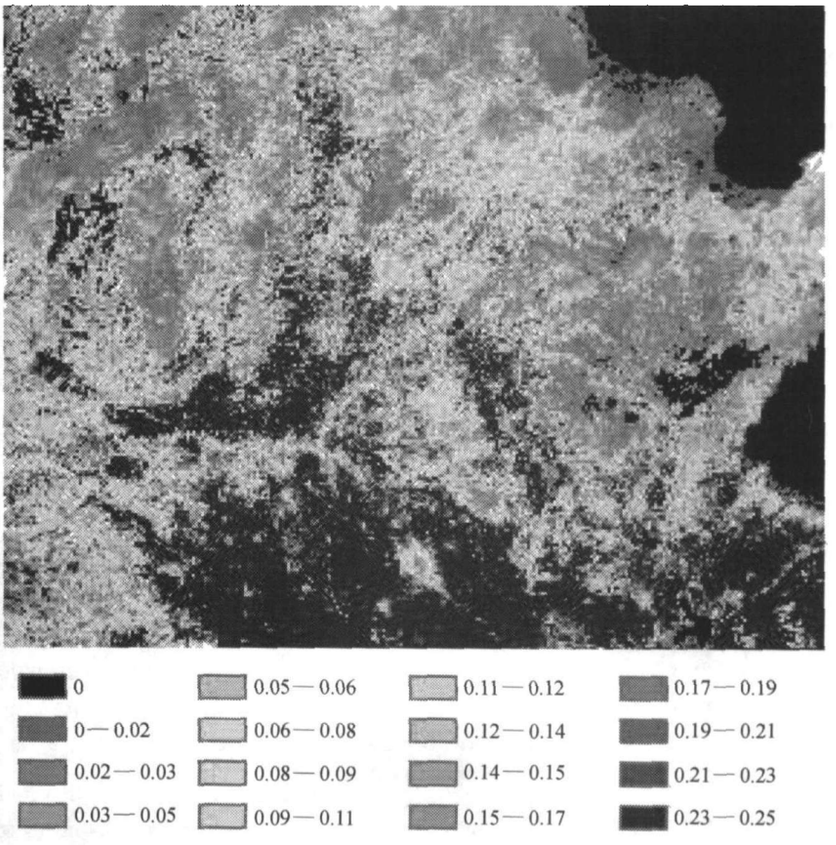

Fig. 8. Regional distribution image of vegetation carbon dioxide assimilation flux.

pixel was separated by establishing thermal inertia information, while in this paper by PCACA algorithm; in the former, the net radiation flux was separated by Beer's Law, the vegetation transpiration was calculated by the residual term method, but in this paper by layered energy-separating algorithm. Therefore, after the establishment of the more perfect calibration fields of the dry point and the wet point, the model and the algorithm proposed in this paper must have some applied potentials. At present, before the establishment of the two calibration fields, we shall use these two models at the same time and make full use of their respective advantages.

5 Conclusions and discussions

(1) The PCACA algorithm was proposed in this paper. The specific steps of the algorithm include: first, to separate the component temperature of the mixed pixel, furthermore, combining with the observed values of the dry points and the wet points in the calibration fields to calculate the true temperatures of the four extreme mixed pixels, thus confirming the trapeziform frame under the weather and ecological conditions of the given time; second, we gained the slope dT_m/df by the absolute dry line and wet line, and analyzed the hypothesis of the PCACA algorithm with which to separate the temperature of the mixed pixel. This algorithm suggests that the coupling mechanism of the soil and the vegetation canopy in PCACA is not the same as the patch two-layer model's, but the same as the improved two-layer model's. Under this hypothesis, there are transitional soil iso-moisture lines between the dry line and the wet line, which are the same lines as the iso-slope lines. The idea of this paper is consistent with the experimental results of Carlson and Moran[24—26]. With this algorithm, the necessary resistance data used in the calculation are reduced from all pixels to four extreme points, and the data of the four points can be obtained from the observations in the calibration fields, which indicates that the algorithm strides a large step from non-operation to operation.

The uncertainty of the hypothesis is large when the mechanism of the patch two-layer model appears, in which there are large area patches of soil and vegetation and soil patches have different soil moisture from vegetation patch. For example, the patch two-source parallel model can be used in the pixels where the villages and the farmlands or the bare lands and lakes occupy similar proportions of the pixel. In this case, the PCACA model of this paper could lead to a large error, but fortunately, according to the sample test for the actual land cover, the proportion of the pixels with the two situations above is only about 10%.

(2) This paper proposes a theoretic positioning algorithm, with which the localization reliability of the dry line and the wet line can be improved, and the uncertainty of PCACA can be conquered. (The uncertainty was caused by the distortion of the up-envelop line and the low-envelop line because of the missing of the dry and wet states and the VFC distribution of the pixels.)

Because, at present, no calibration fields for dry points and wet points can be used, in this paper the results calculated from the observed data of the county meteorology stations near to the four extreme points are inaccurate to some degree. And when the two hypotheses are not tenable that there are two linear relationships and the soil and the vegetation have the same water source, there is some uncertainty.

(3) On the basis of the feasibility of the one-layer energy-separating algorithm, which had been verified by us using the experiment in Tengger desert of western China[30], and the feasibility of the vegetation net radiation-separating algorithm, which had been verified by Norman in N95 model, this paper proposes a two-layer energy-separating algorithm. Here, no horizontal advection is his premise. This algorithm is very simple, has a certain physical foundation, and gets rid of the flux resistance network parameters that are difficult to obtain one by one. In many models, the resistance network expressions were so complex that these models cannot be used.

Analyzed from the traditional points, the uncertainty of this algorithm is due to its ignorance for the influence of the advection. But the heterogeneous sur-

face and the heterogeneous atmosphere caused by surface-atmosphere interactions are the sources of the horizontal advection's influence. Moreover, horizontal advection has a close relationship between the speed and the scale of atmospheric denaturalization. The spatial resolution of MODIS, NOAA-AVHRR in thermal band is 1.1 km×1.1 km. We have a new optimistic concept for the impacts of the advection on the average surface temperature and the net radiation flux obtained in this pixel scale, that for 200 m fetch, the advection only affects the edge of the pixels and inside the pixels, the advection's effects are not so important, because of the mixed and averaged effects and can be expressed using an averaged values for heterogeneous surface. Of course, it is necessary to do the further experiment on the advection's impacts.

(4) In this paper, the albedo of mixed pixel was separated using PCACA algorithm, and combining with the two-layer layered energy-separating algorithm, the net radiation of mixed pixels was separated, which reduces the uncertainty of separating the net radiation flux with Beer's Law.

(5) After the establishment of the calibration fields for dry points and wet points in pixel scale, the model and the algorithm proposed in this paper will have a bright applied prospect.

6 Concluding remarks

The difficulty in retrieving regional surface flux using quantitative remote sensing method is the acquisition of the parameters that cannot be directly measured by remote sensing, such as air temperature, wind speed, roughness length, etc. It has been 30 years from the appearance of the infrared thermal radiometer and the proposal of the simplest correlative equation of the evaporation and the infrared temperature in the middle of 1970s, to the present development of various complicated quantitative remote sensing models. Those who want to make some contributions in regional scale find out some useful information from infrared radiative temperature and vegetation index. The greatest characteristic of SEBAL model is no requirement for air temperature. The model established an empirical relationship between the air temperature and the surface infrared radiative temperature. If the coefficients of the empirical equation are uniform for each pixel, the independent information is still the infrared radiative temperature. The greatest characteristic of the N95 two-source model is that the vegetation transpiration of every pixel can be retrieved. In N95 model, vegetation transpiration is regarded as the function of the VFC and the slope of the saturation vapor pressure-temperature curve, and the vegetation net radiation flux. That is to say, the Bowen Ratio composed of the slope and the VFC is used to divide the vegetation net radiation flux and the slope depends on the surface temperature. Thus, the independent information sources of this model are also the infrared radiative temperature and the vegetation index. We can understand their idea completely, because for optical remote sensing, there is no other information that can support the retrieval of the pixel by pixel besides the two kinds of information sources. Someone proposed that surface flux in regional scale could be retrieved by the decline or the growth of the boundary layer height[31]. But it is impossible to require the sounding balloon data for every pixel. Therefore, Carlson found out the essence and the reality. He calculates the regional surface flux directly using infrared radiative temperature and vegetation index. Carlson appraised his method objectively that it was not perfect but advisable very much[24]. As a senior scientist of America in the field of numerical simulation and prediction, he has such recognition that the above idea should be regarded as our good reference. In this paper, some new methods and ideas were put forward to be references for scholars with interest.

References

1. Price, J. C., Estimation of regional scale evapotranspiration through annalist's satellite thermal infrared data, IEEE Transaction on Geoscience and Remote Sensing, 1982, GE-20: 286—292.
2. Jackson, R. D., Hatfield, J. L., Reginato, R. J. et al., Estimation of daily evapotranspiration from one time-of-day measurements, Agricultural Water Management, 1983, 7: 351—362.
3. Zhang, Renhua, A new model for estimating crop water deficiency based on infrared in6ormation Scientia Sinica, Science in China, Series B, 1987, 30(4): 413—425.
4. Friedl, M. A., Modeling land surface fluxes using a sparse canopy model and radiometric surface temperature measurements, J. Geophysics Res., 1995, 100: 25435—25446.

5. Chehbouni. A., Nichols, W. D., Njoku, E. G et al., A three component model to estimate sensible heat flux over sparse shrubs in Nevada, Remote Sensing Rev., 1997, 15: 99—112.
6. Kalma, J. D., Jupp, D. L. B., Estimating evaporation from pasture using infrared thermometry: evaluation of a one-Layer resistance model, Agricultural and Forest Meteorology, 1990, 51: 223—246.
7. Nichols, W. D., Energy budgets and resistances to energy transport in sparsely vegetated rangeland, Agricultural and Forest Meteorology, 1992, 60: 221—247.
8. Bastiaanssen, W. G. M., Menenti, M., Feddes, R. A. et al., A remote sensing surface energy balance algorithm for land (SEBAL) 1, Formulation, Journal of Hydrology., 1998, 3: 198—212.
9. Su, Z., The surface enerhy system (SEBS) for estimation of turbulent heat fluxes, Hydrology and Earth System Science, 2002, 6(1): 85—99.
10. Deardorff, J. W., Efficient prediction of ground surface temperature and moisture, with inclusion of a layer of vegetation, Journal of Geophysical Research, 1978, 83: 1889—1903.
11. Dickson, O. T., Modeling evapotranspiration for three-dimension global climate model, Geophysics, Monograph, 1984, 29: 58—72.
12. Shuttleworth, W. J., Wallace, J. S., Evaporation from sparse crop-an energy combination theory, Q. J. R. Metrology, Soc., 1985, 111: 839—855.
13. Choudhury, B. J., Monteith, J. L., A four-layer model for the heat budget of homogenous land surface, Q. J. R. Metrology, Soc., 1988, 114: 373—398.
14. Choudhury, B. J., Estimation evaporation and carbon assimilation using infrared temperature data: vistas in modeling, In: Asrar, G, ed. John Wiley., Theory and Applicatons of Remote Sensing, New York: New York Press, 1989, 628—690.
15. Norman, J. M., Kustas, W. P., Humes, K., Source approach soil and vegetation energe flux in observation of directional radiometric surface temperature, Agriculture and Forest Meteorology., 1955, 77: 263—293.
16. Kustas, W. P., Choudhury, B. J., Moran, M. S. et al., Determination of sensible heat flux over sparse canopy using thermal infrared data, Agricultural and Forest Meorology, 1989, 44: 197—216.
17. Kustas, W. P., Norman, J. M., Evaluation of soil and vegetation heat flux prediction using a simple two-source model with radiometric temperature for canopy cover, Agricultural and Forest Meorology, 1999, 94: 13—29.
18. Kustas, W. P., Norman, J. M., A two-source energy balance approach using directional radiometric temperature observation for sparse canopy covered surface, Agrinomy Journal, 2000, 92: 847—854.
19. Kustas, W. P., Timmermans, W. J., French, A. N., An intercomparison of two remote sensing-based energy balance modeling schemes, Proceedings of IGARSS04, 2004.
20. Li Zhaoliang, M. P. Stoll, Zhang Renhua., On the separate retrieval of soil and vegetation temperatures from ATSR data, Science in China, Series E, 2001, 44(2): 97—111.
21. Chen Jingming, A Chief detect of modern remote sensing evapotranspiration model and its improvement, Chinese Science Bulletin (in Chinese), 1988, 33(6): 454—458.
22. Zhang Renhua, Sun Xiaomin, Zhu Zhilin et al., A remote sensing model of CO2 flux for wheat and studying of regional distribution, Science in China, Series D, 1999, 42(3): 325—336.
23. Zhang Renhua, Sun Xiaomin, Liu Jiyuan et al., Determination of regional distribution of crop transpi ration and soil water use efficiency using quantitative remote sensing data through inversion, Science in China, Series D, 2003, 46(1): 10—22.
24. Carlson, T. N., William, C., Rjobert, J. G., A New Look at the Simplified Method for Remote Sensing of Daily Evapotranspiration, Remote Sensing of Environment., 1995, 54: 161—167.
25. Moran, M. S., Clarke, T. R., Inoue, Y. et al., Estimating crop water deficit using the relation between surface -air temperature and spectral vegetation index, Remote Sensing of Environment, 1994, 49: 246—263.
26. Moran, M. S., Humes, K. S., Pinter, Jr. P. J., The scaling characteristics of remotely-sensed variables for sparsely-vegetated heterogeneous landscapes, Journal of Hydrology, 1997, 190: 337—362.
27. Priestley, C. H. B., Taylor, R. J., On the assessment of surface heat flux and evaporation using large scale parameters, Monthly Weather Review, 1972, 100: (2): 81—92.
28. Zhang Renhua, Experimental Remote Sensing Modeling and Surface Foundations (in Chinese), Beijing: Science Press, 1996.
29. Kimes, D. S., View angle effects in the radiometric measurement of plant canopy temperatures, Remote Sensing of Environment, 1980, 10: 273—28.
30. Zhang Renhua, Sun Xiaomin, Zhu Zhilin et al., A remote sensing model for monitoring soil evaporation based on differential thermal inertia and its validation, Science in China, Series D, 2003, 46 (4): 344—355.
31. Anderson, M. C., Norman, J. M., Diak, G. R. et al., A two-source time-integrated model for estimating surface fluxes using thermal infrared remote sensing, Remote Sensing of Environment, 1997, 60: 195—216.